1971MNRAS.153..471B

Mon. Not. R. astr. Soc. (1971) **153**, 471–490.

CALCULATIONS OF THE LEVEL POPULATIONS FOR THE LOW LEVELS OF HYDROGENIC IONS IN GASEOUS NEBULAE

M. Brocklehurst

(Communicated by M. J. Seaton, F.R.S.)

(Received 1971 April 28)

Downloaded from https://academic.oup.com/mnras/article/153/4/471/2604558 by guest on 20 August 2022

SUMMARY

The level populations, b_{nl} of hydrogen and singly ionized helium are calculated making full allowance for collisional redistribution of angular momentum and energy. In many cases the l-states are not populated statistically. Intensities of the most important line series are presented for $n \leqslant 40$ and for a wide range of electron temperatures and electron densities. Calculated relative intensities in the spectra of H I are compared with observed intensities in the planetary nebula NGC 7662. The agreement with the photoelectric observations is good, but there is poor agreement with the photographic observations.

1. INTRODUCTION

The recombination spectra of H^+ regions have been calculated using various simplifying assumptions (Burgess 1958; Seaton 1960; Pengelly 1964). For a well observed bright nebula, up to 40 lines may be observed in the optical recombination spectra* of H I, He I and He II. There has been considerable interest in comparing the observations with calculations (Kaler 1966).

The determination of the spectrum produced by an assembly of electrons and bare nuclei (mainly protons), due to the processes of radiative capture and cascade, was first made by Plaskett (1928). Solutions were obtained for an atom with a finite number of levels, and it was implicitly assumed that, for a given value of the principal quantum number, n, the populations of the degenerate quantum states nl were proportional to their statistical weights $\omega_{nl} = 2(2l+1)$;

$$N_{nl} = N_n \frac{(2l+1)}{n^2} \tag{1.1}$$

where N_i is the number of atoms per unit volume in state i. Such population distributions will be referred to as statistical. Assuming (1.1), Baker & Menzel (1938) obtained solutions for an infinite number of levels by an iterative scheme, whilst Seaton (1959) obtained similar solutions using the more elegant cascade matrix technique.

The agreement with observations was poor for high lines, the observed intensities being greater than the calculated intensities (Seaton 1960; Kaler 1966). This

* Regions of ionized hydrogen emit the H I spectrum. We therefore refer to 'H^+ regions', in preference to the more common term 'H II regions'. This is consistent with the 1952 resolution of I.A.U. Commission 34 (*I.A.U. Transactions*, Vol. VIII, p. 527).

© Royal Astronomical Society • Provided by the NASA Astrophysics Data System

1971MNRAS.153..471B

led Seaton to suggest that systematic errors were present in the observations, but careful new observations by Aller, Bowen & Wilson (1963) appeared to confirm the earlier results of Aller, Bowen & Minkowski (1955).

In the above calculations there is a discontinuity in the physical conditions assumed, in that collisional processes which are ignored for bound states must become important for large n, while it is assumed that the free electrons are collisionally dominated and form a Maxwellian distribution. Seaton (1964) allowed partially for the redistribution of energy by electron–atom collisions, and Brocklehurst (1970) (hereafter referred to as Paper I) allowed fully for all such processes. They were found to have only a small effect upon the less excited states ($n < 40$), and could not explain the above discrepancies.

Equation (1.1) will be valid when collisional processes leading to a redistribution of angular momentum are very much faster than radiative processes. There will always be a level n, above which this holds true, and the calculations of Paper I (the n-method) are valid. The calculations for the less excited states are certainly incorrect, however, and the intensities of the Balmer series and other important transitions of astrophysical interest will be wrongly predicted. Extensive calculations were made by Pengelly (1964) assuming no collisional redistribution of angular momentum or of energy. A re-analysis of the observations indicated that the nl-method was in worse agreement with experiment than the n-method (Kaler 1966, 1968).

It would appear that some process not considered in the calculations is maintaining a statistical distribution amongst the l-states. Pengelly & Seaton (1964) showed that the collisional processes for redistribution of angular momentum could have large cross-sections even for small values of n. The calculations presented below allow exactly for such processes, induced by protons and other charged particles, and also for the less important process of collisional redistribution of energy. The level populations, calculated for a wide range of physical conditions and for both hydrogen and singly ionized helium are found to depart radically from the statistical distribution. As expected, the line intensities of the principal series lie between the n-method calculations (valid in the limit of large densities) and the nl-calculations of Pengelly (valid in the limit of zero density).

The paper concludes with a comparison of the theoretical and observed line intensities of NGC 7662. The agreement with the photo-electric observation of high Balmer lines (Miller 1971) is very good. It is suggested that intensities obtained photographically contain systematic errors.

2. FORMULATION

The level populations are conveniently described by the usual b factors. Thus the Saha equation is written

$$N_{nl} = N_+ N_e \left(\frac{h^2}{2\pi mkT_e}\right)^{3/2} \frac{\omega_{nl}}{2}\, e^{x_{nl}} b_{nl}. \qquad (2.1)$$

Where $x_{nl} = I_{nl}/kTe$, I_{nl} is the ionization energy of level nl (which is independent of l for hydrogenic systems), N_e is the electron density and N_+ is the ion density. For thermodynamic equilibrium $b_{nl} = 1$ and, with a Maxwellian distribution,

Downloaded from https://academic.oup.com/mnras/article/153/4/471/2604558 by guest on 20 August 2022

© Royal Astronomical Society • Provided by the NASA Astrophysics Data System

1971MNRAS.153..471B

$b = 1$ for free electron states. We note that

$$\sum_l N_{nl} = N_n$$

and equation (1.1) implies $b_{nl} = b_n$.

Baker & Menzel (1938) formulated two distinct cases in the determination of the spectrum. In Case A it is assumed that the ground state is depopulated by photoionization processes alone, whilst in Case B it is assumed that the rate of depopulation of an excited state by the emission of Lyman quanta is balanced by the rate of population due to absorption of Lyman quanta. In this case, the level $2p$ is metastable and the population will increase until absorption of Balmer quanta becomes important. Osterbrock (1962) has shown, however, that, for an isolated nebula, a Ly-α quantum will escape or be absorbed by conversion to two quanta after 10^7 scatterings, and the $2p$ population does not become significant.

The dominant physical processes occurring under conditions typically found in gaseous nebulae are radiative recombination, radiative cascade, collisional redistribution of energy by electrons and collisional redistribution of angular momentum by ions. Collisional ionization and the inverse process, three body recombination, are negligible for levels $n<40$. Similarly, for any known H^+ region, the effects of the free–free radiation field are negligible (Dyson 1969). Equating processes which populate and depopulate a quantum level nl, we have

$$N_e N_+ \alpha_{nl} + \sum_{n'=n+1}^{\infty} \sum_{l'=l\pm1} A_{n'l',\,nl} N_{n'l'}$$

$$+ \sum_{l'=l\pm1} N_e N_{nl'} C_{nl',\,nl} + \sum_{n'=n_0}^{\infty} \sum_{l'=l\pm1} N_e N_{n'l'} C_{n'l',\,nl}$$

$$= N_{nl}\left[A_{nl} + \sum_{l'=l\pm1} N_e C_{nl,\,nl'} + \sum_{n'=n_0}^{\infty} \sum_{l'=l\pm1} N_e C_{nl,\,n'l'}\right]. \qquad (2.2)$$

For the ground state it is necessary to include photoionization of ground state atoms by stellar ultra-violet radiation. For Case A, $n_0 = 1$ and for Case B, $n_0 = 2$. The radiative recombination coefficient for nl is α_{nl} and the radiative transition probability for $n'l' \to nl$ is $A_{n'l',\,nl}$. A_{nl} is the total radiative transition probability for nl and is given by

$$A_{nl} = \sum_{n''=n_0}^{n-1} \sum_{l''=l\pm1} A_{nl,\,n''l''}. \qquad (2.3)$$

The collision rates, $C_{nl',\,nl}$ for redistribution of angular momentum and $C_{n'l',\,nl}$ for redistribution of energy are defined such that

$$C_{i,\,j} = \int Q_{ij} v f(v)\, dv \qquad (2.4)$$

where $f(v)$ is a Maxwellian velocity distribution. From detailed balancing considerations we find

$$e^{x_i} \omega_i C_{i,\,j} = e^{x_j} \omega_j C_{j,\,i}. \qquad (2.5)$$

Substituting (2.1) and (2.5) in (2.2), we obtain the equilibrium equation in

30

© Royal Astronomical Society • Provided by the NASA Astrophysics Data System

Downloaded from https://academic.oup.com/mnras/article/153/4/471/2604558 by guest on 20 August 2022

1971MNRAS.153..471B

terms of the b_{nl} factors.

$$\sum_{n'=n+1}^{\infty} \mathrm{e}^{x_{n'}}\left(\sum_{l'=l\pm1} (2l'+1)\, A_{n'l',\, nl} b_{n'l'}\right) - (2l+1)\, A_{nl}\, \mathrm{e}^{x_n} b_{nl}$$
$$+\mathrm{e}^{x_n}(2l+1)\left(\sum_{n'=n_0}^{\infty} \sum_{l'=l\pm1} N_e C_{nl,\, n'l'} b_{n'l'} - b_{nl} \sum_{n'=n_0}^{\infty} \sum_{l'=l\pm1} N_e C_{nl,\, n'l'}\right)$$
$$+\mathrm{e}^{x_n}(2l+1)\left(\sum_{l'=l\pm1} N_e C_{nl,\, nl'} b_{nl'} - b_{nl} \sum_{l'=l\pm1} N_e C_{nl,\, nl'}\right)$$
$$= -\alpha_{nl}\left(\frac{h^2}{2\pi mkT_e}\right)^{-3/2}. \quad (2.6)$$

The method of solving (2.6) will be discussed in Section 4.

3. THE EVALUATION OF THE RATE COEFFICIENTS

(i) *Radiative coefficient* $A_{nl,\, n'l'}$

The spontaneous transition probability $A_{nl,\, n'l'}$ for electric dipole radiation in hydrogen and hydrogenic ions is given by

$$A_{nl,\, n'l'} = \frac{64\pi^4\nu^3}{Z^2 3hc^3} \frac{\max(l, l')}{(2l+1)}\, e^2 a_0{}^2 \left[\int_0^\infty R(n'l')\, rR(nl)\, dr\right]^2 \quad (3.1)$$

where

$$a_0 = \hbar^2/me^2 \quad (3.2)$$

and

$$\nu = cRZ^2\left(\frac{1}{n'^2} - \frac{1}{n^2}\right) \quad (3.3)$$

is the frequency of the transition $n'l' \to nl$ and $R(nl)$ is the normalized radial wave function. On substituting in (3.1) for ν and rearranging

$$A_{nl,\, n'l'} = 2{\cdot}6774\ 10^9\ Z^4 a_{nl,\, n'l'} \quad (3.4)$$

where

$$a_{nl,\, n'l'} = \left(\frac{1}{n'^2} - \frac{1}{n^2}\right)^3 \frac{\max(l, l')}{(2l+1)} |\rho(n'l', nl)|^2 \quad (3.5)$$

and

$$\rho(n'l', nl) = \int_0^\infty R(n'l')\, rR(nl)\, dr. \quad (3.6)$$

The tables of radial integrals $|\rho|^2$ published by Green, Rush & Chandler (1957) are not extensive enough. For $n \leqslant 40$ we compute the values using the expression given by Gordon (1929):

$$|\rho(n'l-1, nl)|^2 = \left\{\frac{(-1)^{n'-l}}{4(2l-1)!} \sqrt{\frac{(n+l)!\,(n'+l-1)!}{(n-l-1)!\,(n'-l)!}} \frac{(4nn')^{l+1}}{(n+n')^{n+n'}}\right.$$
$$\times (n-n')^{n+n'-2l-2}\left[{}_2F_1\left(-n+l+1,\, -n'+l,\, 2l,\, \frac{-4nn'}{(n-n')^2}\right)\right.$$
$$\left.\left. - \left(\frac{n-n'}{n+n'}\right)^2 {}_2F_1\left(-n+l-1,\, -n'+l,\, 2l,\, -\frac{4nn'}{(n-n')^2}\right)\right]\right\}^2 \quad (3.7)$$

Downloaded from https://academic.oup.com/mnras/article/153/4/471/2604558 by guest on 20 August 2022

© Royal Astronomical Society • Provided by the NASA Astrophysics Data System

1971MNRAS.153..471B

where ${}_2F_1$ is the hypergeometric function. When (3.7) is being used to evaluate the matrix elements, the convention is adopted that if the l-value of the upper state is the larger, the total quantum number for this state is represented by n. If the l-value for the upper state is smaller, the quantum number for this state is n'. Finally, the leading term in (2.6) requires the evaluation of an infinite sum involving A coefficients. To this end, asymptotic expressions for $A_{n'l',\,nl}$, $n' \to \infty$ will be derived in Section 3 (iii).

(ii) *Recombination coefficient* α_{nl}

We require the rate coefficients α_{nl} for the capture of a free electron by an ion, to give an atom or ion of one less charge in some final state nl. Consider, first, the ionization of an hydrogenic ion of nuclear charge Z by a photon of energy $h\nu$. The electron, initially in a state nl is ejected with an energy k^2, such that

$$h\nu = \left(\frac{Z^2}{n^2}+k^2\right) I_H. \tag{3.8}$$

The photoionization cross-section a_{nl} for this process is given by Burgess & Seaton (1960)

$$a_{nl}(k^2) = \left(\frac{4\pi\alpha a_0{}^2}{3}\right)\frac{n^2}{Z^2}\sum_{l'=l\pm 1}\frac{\max(l,\,l')}{(2l+1)}\,\Theta(nl,\,Kl') \tag{3.9}$$

where

$$\Theta(nl,\,Kl') = (1+n^2K^2)\,|g(nl,\,Kl')|^2 \tag{3.10}$$

$$g(nl,\,Kl') = \frac{Z^2}{n^2}\int_0^\infty R_{nl}(r)\,rF_{Kl}(r)\,dr \tag{3.11}$$

and where

$$\alpha = 2\pi e^2/ch \tag{3.12}$$

is the fine structure constant, l' is the angular momentum quantum number of the ejected electron and $K = k/Z^2$. In equation (3.11), $R_{nl}(r)$ and $F_{kl}(r)$ are the initial and final radial wave functions of the ejected electron, F_{kl} being normalized to asymptotic amplitude $k^{-1/2}$.

The recombination coefficient is obtained from the photoionization cross-sections. With a Maxwellian velocity distribution corresponding to an electron temperature T_e°K, we have (Burgess 1965)

$$\alpha_{nl} = \left(\frac{2\pi^{1/2}\alpha^4 a_0{}^2 c}{3}\right)\frac{2y^{1/2}}{n^2}\,Z\sum_{l'=l\pm 1} I(n,\,l,\,l',\,t) \tag{3.13}$$

where

$$I(n,\,l,\,l',\,t) = \max(l,\,l')\,y\int_0^\infty (1+n^2K^2)^2\,\Theta(nl,\,Kl')\,e^{-K^2 y}\,d(K^2) \tag{3.14}$$

and

$$y = Z^2Rhc/kT_e = 15.778/t \tag{3.15}$$

with

$$t = T_e/10^4Z^2. \tag{3.16}$$

Many evaluations of Θ are necessary, requiring expressions amenable to rapid computation. The radial wave functions may be expressed in terms of hypergeometric functions but this procedure becomes unsuitable for large n. Following

Downloaded from https://academic.oup.com/mnras/article/153/4/471/2604558 by guest on 20 August 2022

© Royal Astronomical Society • Provided by the NASA Astrophysics Data System

1971MNRAS.153..471B

the suggestion of Burgess (1965), we write

$$g(nl, Kl') = \sqrt{\frac{(n+l)!}{(n-l-1)!}\prod_{s=0}^{l'}(1+s^2K^2)}\,(2n)^{l-n}\,G(n, l, K, l') \tag{3.17}$$

and obtain

$$G(n, n-1, 0, n) = \sqrt{\frac{\pi}{2}}\,\frac{8n}{(2n-1)!}\,(4n)^n\,e^{-2n} \tag{3.18}$$

$$G(n, n-1, K, n) = \frac{1}{\sqrt{1-e^{-2\pi/K}}}\,\frac{\exp\,(2n-2/K\,\tan^{-1}\,(nK))}{(1+n^2K^2)^{n+2}} \times G(n, n-1, 0, n) \tag{3.19}$$

$$G(n, n-2, K, n-1) = (2n-1)(1+n^2K^2)\,nG(n, n-1, K, n) \tag{3.20}$$

$$G(n, n-1, K, n-2) = \left(\frac{1+n^2K^2}{2n}\right)G(n, n-1, K, n) \tag{3.21}$$

$$G(n, n-2, K, n-3) = (2n-1)(4+(n-1)(1+n^2K^2))\,G(n, n-1, K, n-2). \tag{3.22}$$

The recurrence relations for G are

$$\begin{aligned} G(n, l-2, K, l-1) = {} & [4n^2-4l^2+l(2l-1)(1+n^2K^2)]G(n, l-1, K, l) \\ & -4n^2(n^2-l^2)[1+(l+1)^2K^2]G(n, l, K, l+1) \end{aligned} \tag{3.23}$$

$$\begin{aligned} G(n, l-1, K, l-2) = {} & [4n^2-4l^2+l(2l+1)(1+n^2K^2)]G(n, l, K, l-1) \\ & -4n^2[n^2-(l+1)^2](1+l^2K^2)G(n, l+1, K, l). \end{aligned} \tag{3.24}$$

Repeated application of equations (3.23) and (3.24) involves nothing more complicated than multiplication and is ideally suited for rapid computing. Equation (3.14) was not evaluated by the Gauss–Laguerre method since it was found that unless a large number of integration points were employed, a sizeable part of the integral could lie between the first two points or even before the first point. An ordinary Gaussian quadrature scheme was adopted, with an upper cut off $K_{\max}$ such that

$$\Theta(n, l, K_{\max}, t) = 10^{-5}\,\Theta(n, l, 0, t). \tag{3.25}$$

Variation of the accuracy parameter in the case of worst convergence ($l = 0$, t large) indicated that the final integrals, I, were accurate to at least 4 figures. Burgess (1965) discussed the possibilities of errors building up during repeated use of the recurrence relations. No differences in the final values were found when computed using 64-bit words on the University College London IBM 360/65 or using 48-bit words on the University of London CDC 6600.

(iii) *Asymptotic form of the radiative coefficients*

For the purpose of evaluation of the term

$$\sum_{n'=n+1}^{\infty} A_{n'l',\,nl}(2l'+1)b_{n'l'},$$

it is necessary to know the form of the radiative coefficient at large n'. We may write expressions for the free and bound radial wave functions of the electron

Downloaded from https://academic.oup.com/mnras/article/153/4/471/2604558 by guest on 20 August 2022

© Royal Astronomical Society • Provided by the NASA Astrophysics Data System

1971MNRAS.153..471B

in the limits of zero energy k and infinite quantum number n', respectively

$$F_{kl'}(r) \xrightarrow{k\to 0} \sqrt{\frac{\pi}{2}} \frac{(2Zr)^{l'+1}}{(2l'+1)!} Z^{-1/2} \tag{3.26}$$

$$R_{n'l'}(r) \xrightarrow{n'\to\infty} \frac{(2Zr)^{l'+1}}{n'^{3/2}} \frac{Z^{1/2}}{(2l'+1)!}. \tag{3.27}$$

Since (3.26) and (3.27) have the same r dependence, it follows from (3.7) and (3.11) that

$$\frac{\rho}{g} \to \frac{n^2}{Z} \sqrt{\frac{2}{\pi}}\, n'^{-3/2} \tag{3.28}$$

and hence

$$n'^3 A_{n'l',\,nl} \xrightarrow{n'\to\infty} 2\cdot6774.10^9 \left(\frac{2}{\pi}\right) \frac{\max(l,\, l')}{(2l'+1)} \frac{\Theta_{nl,\,0l'}\, Z^2}{n^2}. \tag{3.29}$$

The quantity required in the solutions of the equilibrium equations is

$$\sum_{l'=l\pm1} (2l'+1) A_{n'l,\,nl} = T.$$

From (3.29) we have

$$n'^3 T \to \frac{2\cdot6774}{n^2}.10^9 \left(\frac{2}{\pi}\right)\{(l+1)\,\Theta_{nl,\,0l+1} + l\Theta_{nl,\,0l-1}\}. \tag{3.30}$$

(iv) *Collision cross-sections*

The semi-classical impact parameter method (Seaton 1962) is ideally suited to calculating reaction rates for optically allowed transitions between states of very small energy separation. For excitation by a particle of velocity v and charge z, the cross-section is

$$Q = \int_0^\infty 2\pi\rho P(\rho)\, d\rho \tag{3.31}$$

where ρ is the impact parameter and P is a transition probability. Introducing a lower cut off ρ_1 in the impact parameter we obtain

$$Q = \tfrac{1}{2}\pi\rho_1^2 + Q_1 \tag{3.32}$$

where

$$Q_1 = \frac{8\pi z^2 e^2}{3\hbar^2} \frac{S}{v^2} \ln(1\cdot12\hbar v/\rho_1 \Delta E) \tag{3.33}$$

and S is the line strength of the transition.

For transitions of the type $n \to n \pm 1$, a large contribution to the cross-sections comes from impact parameters $\rho > \rho_1$, and the cross-sections are very accurate (Saraph 1964).

For transitions of the type $nl \to nl'$ induced in hydrogenic ions by ionic impact, $\Delta E = 0$ and equation (3.33) leads to infinite cross-sections. Pengelly & Seaton (1964) introduced an upper cut-off ρ_c in the impact parameter to obtain finite cross-sections:

$$Q_1 = \frac{8\pi z^2 e^2 S}{3\hbar^2 v^2} \ln(\rho_c/\rho_1). \tag{3.34}$$

Downloaded from https://academic.oup.com/mnras/article/153/4/471/2604558 by guest on 20 August 2022

© Royal Astronomical Society • Provided by the NASA Astrophysics Data System

1971MNRAS.153..471B

Allowing for the possibility of the atom radiating during the encounter gives

$$\rho_c \sim 0 \cdot 72\, \tau v \tag{3.35}$$

where τ is the radiative lifetime. Alternatively, the effective range of the Coulomb field of the ions may be reduced by the electrons clustering around the ions. Spitzer (1956) gives

$$\rho_D = \left(\frac{kT_e}{4\pi^2 N_e e^2}\right)^{1/2} \tag{3.36}$$

where N_e is the electron density. The smaller of ρ_c and ρ_D is chosen. Since equation (3.34) indicates that the cross-sections for redistribution of angular momentum depend only upon the velocity of the colliding particle, we can neglect collisions with electrons.

(v) *Collision rates*

A re-evaluation of the collision rates for redistribution of angular momentum, as defined by (2.4), leads to the following expressions

$$C_{nl} = C_{nl,\, nl+1} + C_{nl,\, nl-1} \tag{3.37}$$

$$C_{nl} = 9 \cdot 933\ 10^{-6} \left(\frac{\mu}{m}\right)^{1/2} \frac{D_{nl}}{T_e^{1/2}} N_e \left\{11 \cdot 538 + \log_{10}\left(\frac{T_e m}{D_{nl}\mu}\right) + 2 \log_{10} \rho_c\right\} \tag{3.38}$$

where

$$D_{nl} = \left(\frac{z}{Z}\right)^2 6n^2(n^2 - l^2 - l - 1) \tag{3.39}$$

and μ is the reduced mass of the colliding system. For $\rho_c = \rho_D$ we have

$$2 \log_{10} \rho_c = 1.181 + \log_{10}(T_e/N_e) \tag{3.40}$$

and for $\rho_c = 0 \cdot 72\, \tau v$

$$2 \log_{10} \rho_c = 10 \cdot 95 + \log_{10}\left(\frac{m T_e \tau^2}{\mu}\right). \tag{3.41}$$

It is essential that individual collision rates obtained from (3.37) obey the detailed balancing principle (2.5). By commencing at $l = 0$, we have, from (3.37)

$$C_{n0,\, n1} = C_{n0}. \tag{3.42}$$

Alternate application of (3.37) and (2.5), using (3.42) as a starting value gives the values of $C_{nl,\, nl+1}$ for all l. Similarly, by starting at $l = n-1$ we have

$$C_{nn-1,\, nn-2} = C_{nn-1} \tag{3.43}$$

and an identical process again gives $C_{nl,\, nl+1}$. The two sets of values are different since ρ_c is l-dependent. For $n > 5$, however, the two values agree to within two per cent, the agreement rapidly improving with increasing n. The average value of $C_{nl,\, nl+1}$ is taken and the coefficients $C_{nl,\, nl-1}$ are obtained from (2.5).

4. SOLUTIONS OF THE EQUILIBRIUM EQUATIONS

There is always some value, n_c, of the principal quantum number n, above which collisional processes are very much faster than radiative processes. We

Downloaded from https://academic.oup.com/mnras/article/153/4/471/2604558 by guest on 20 August 2022

© Royal Astronomical Society • Provided by the NASA Astrophysics Data System

1971MNRAS.153..471B

require

$$\frac{N_e C_{n_c l}}{A_{n_c l}} > 100, \qquad l = 1 \tag{4.1}$$

since the transition probabilities to the ground state are the largest. Hence the l-states will, to a good approximation, be statistically populated, and their populations will be characterized by the b_n coefficients of Paper I. For most cases it is found that $n_c \lesssim 40$. Neglecting, temporarily, the collisional redistribution of energy, the equilibrium equation (2.6) becomes

$$\begin{aligned}
&\sum_{n'=n+1}^{n_c-1} e^{x_{n'}} \left(\sum_{l'=l\pm1} (2l'+1) A_{n'l',\, nl} b_{n'l'} \right) \\
&+ \sum_{n'=n_c}^{n_{\max}-1} e^{x_{n'}} \left(\sum_{l'=l\pm1} (2l'+1) A_{n'l',\, nl} \right) b_{n'} \\
&+ \tfrac{1}{2}\, e^{x_{n_{\max}}} \sum_{l'=l\pm1} (2l'+1) A_{n_{\max}l',\, nl} b_{n_{\max}} \\
&+ I - (2l+1) A_{nl}\, e^{x_n} b_{nl} \\
&+ e^{x_n}(2l+1) \left(\sum_{l'=l\pm1} N_e C_{nl,\, nl'} b_{nl'} - b_{nl} \sum_{l'=l\pm l} N_e C_{nl,\, nl'} \right) \\
&\qquad = -\alpha_{nl} \left(\frac{h^2}{2\pi mkT_e} \right)^{-3/2}
\end{aligned} \tag{4.2}$$

where

$$I = \int_{n_{\max}}^{\infty} e^{x_{n'}} \left(\sum_{l'=l\pm1} (2l'+1) A_{n'l',\, nl} \right) b_{n'} dn'. \tag{4.3}$$

Using (3.30), we put

$$\sum_{l'=l\pm1} b_{n'}(2l'+1) A_{n'l',\, nl} = \left(\frac{1}{n'^3} + \frac{B}{n'^5} + \frac{C}{n'^7} \right) \frac{5{\cdot}348\ 10^9}{\pi} \frac{Z^2}{n^2} \times (l\Theta_{nl,\, 0l-1} + (l+1)\Theta_{nl,\, 0l+1}). \tag{4.4}$$

which has the correct asymptotic form. The coefficients B and C are evaluated on solving the simultaneous equations obtained on setting $n' = n_{\max}$ and $n' = n_{\max}+40$. On substituting (4.4) in (4.3), I may be evaluated analytically, and the total radiative cascade term is obtained.

The value of $n_{\max}$ is determined as follows. Evaluation of the sum of the radiative cascade from levels $n' \gtrsim n_c$ on to the level nl and the radiative recombination on to nl is performed for $n_{\max} = n_c + m\Delta$, $m = 1, 2, 3 \ldots$, where Δ is a suitable step length. Extensive calculations indicate that cascade totals accurate to five parts in 10^4 may be obtained using $\Delta = 5$, and terminating the process when two successive evaluations agree to one part in 10^4. A relatively high accuracy in the cascade total is aimed for, since any errors in the populations would build up as the calculations proceed. It is found that $n_{\max} < 60$ for most states.

In the following calculations we assume that the regions producing the H I spectrum contain only hydrogen. Churchwell & Mezger (1970) obtain helium to hydrogen abundance ratios of 0·1 for many nebulae. Assuming that the helium is singly ionized we have

$$C_{nl} = C_{nl}(\mathrm{H}^+\ \text{impact}) + 0{\cdot}1\ C_{nl}(H_e^+\ \text{impact}). \tag{4.5}$$

Downloaded from https://academic.oup.com/mnras/article/153/4/471/2604558 by guest on 20 August 2022

© Royal Astronomical Society • Provided by the NASA Astrophysics Data System

1971MNRAS.153..471B

Since equation (3.38) indicates that the collision rates are proportional to the square root of the mass of the colliding particle, the total collision rate (4·5) for a nebula with electron density N_e, containing 10 per cent of helium, is equal to that for a pure hydrogen nebula with density $N_e' = N_e \times 1{\cdot}2/(1{\cdot}1)$. The He II spectrum, however, is generally produced in regions where most of the helium is doubly ionized. Adopting the above abundance ratio for all calculations of the He II spectrum, we put

$$C_{nl}(\text{He II}) = C_{nl}(\text{H}^+ \text{ impact}) + 0{\cdot}1\, C_{nl}(\text{He}^{++} \text{ impact}). \tag{4.6}$$

Hence equation (4.2) may be solved for b_{nl} for $n = n_c - 1$. Using these solutions, the departure coefficients may then be obtained for $n = n_c - 2$, and the process is continued until level $n_0 + 1$ is reached. For a fixed n, equation (4.2) leads to a set of simultaneous equations of well-defined character. The coefficients form an $(l \times l)$ band matrix, which is easily handled by digital computers.

It was found, in certain cases, that the computed values of b_{n_c-1l} did not agree too well with the degenerate values b_{n_c-1}. This was caused by neglecting collisional redistribution of energy. The cross sections in Section 3(iv) are only applicable to $n \to n \pm 1$ transitions. Paper I, however, shows that these are the dominant transitions, and we neglect transitions of the type $n \to n'$ $(n' \neq n \pm 1)$. The $n \to n \pm 1$ collisional terms of (2.6) are added to the right-hand side of (4.2). Solutions are obtained in a similar manner, using an iterative scheme. Approximations for the, as yet unknown, values of b_{nl} are used as follows:

(a) First solution

For

$$\left.\begin{array}{ll} n' \geqslant n_c, & b_{nl} = b_n \\ n_c > n' > n, & b_{nl} = b_{nl}^{(1)} \\ n' < n, & b_{nl} = b_n \end{array}\right\} \text{To give solutions } b_{nl}^{(1)} \tag{4.7}$$

(b) First iteration

$$\left.\begin{array}{ll} n' \geqslant n_c, & b_{nl} = b_n \\ n_c > n' > n, & b_{nl} = b_{nl}^{(2)} \\ n' < n, & b_{nl} = b_{nl}^{(1)} \end{array}\right\} \text{To give solutions } b_{nl}^{(2)}. \tag{4.8}$$

In practice, it is found that one iteration is sufficient.

5. RESULTS

Figs 1 and 2 show the variation of b_{nl} with n and l for hydrogen Case B, $T_e = 10^4$°K and $N_e = 10^4\,\text{cm}^{-3}$. The large departures from the statistical populations are well illustrated in Fig. 1. Minima at $l = 2$ are due to the large radiative transition probabilities to the ground stage ($n = n_0$). As collisions between l-states become more important the curves flatten. For $n > 30$ the populations are approaching their statistical values. Fig. 2 shows the effects of collisional redistribution of energy, the populations for $n = 40$ being closer to the L.T.E. values than the $n = 30$ populations.

The quantities usually required in astrophysical applications are the intensities

Downloaded from https://academic.oup.com/mnras/article/153/4/471/2604558 by guest on 20 August 2022

© Royal Astronomical Society • Provided by the NASA Astrophysics Data System

1971MNRAS.153..471B

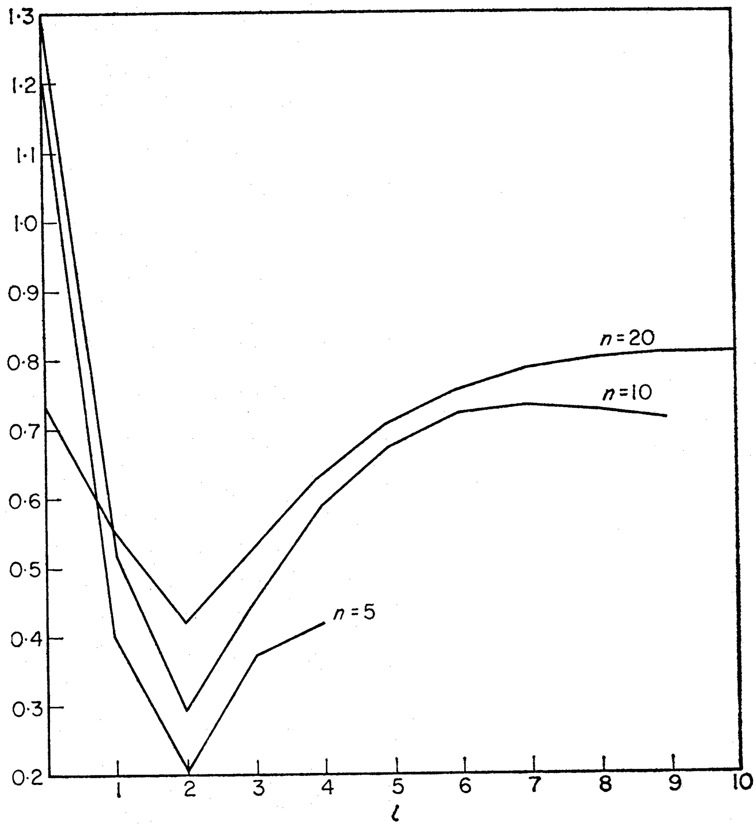

FIG. 1. *The b_{nl} factors for hydrogen Case B, T_e = 10^4°K, N_e = 10^4 cm^{-3}, illustrating the departures from the statistical distribution.*

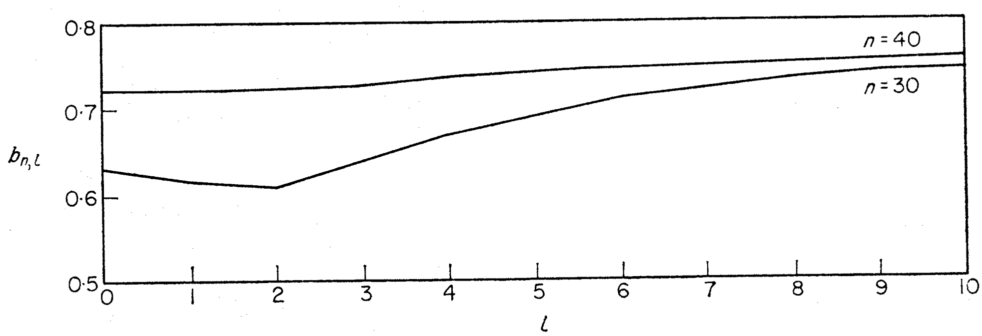

FIG. 2. *The b_{nl} factors for hydrogen Case B, T_e = 10^4°K, N_e = 10^4 cm^{-3}, illustrating the effects of the $n \to n \pm 1$ collisions.*

of the various line series. We have the line emissivity $j_{n,\,n'}$, such that

$$4\pi j_{n,\,n'} = \frac{N_e^2}{T_e^{3/2}}\,0{\cdot}902\ 10^{-26}\left(\frac{1}{n'^2}-\frac{1}{n^2}\right)$$
$$\times\, e^{x_n}\left\{\sum_{l=0}^{n'-1}(2l+1)[A_{nl,\;n'l+1}+A_{nl,\;n'l-1}]b_{nl}\right\}\ \text{erg. cm}^{-3}\,\text{s}^{-1} \qquad (5{\cdot}1)$$

The effective recombination coefficient $\alpha_{n\to n'}$ for the line $n \to n'$ is defined by

$$4\pi j_{n,\,n'} = h\nu_{n,\,n'}N_eN_+\alpha_{n\to n'}(T_e) \qquad (5{\cdot}2)$$

Downloaded from https://academic.oup.com/mnras/article/153/4/471/2604558 by guest on 20 August 2022

© Royal Astronomical Society • Provided by the NASA Astrophysics Data System

1971MNRAS.153..471B

where $\nu_{n,\,n'}$ is the line frequency. The line intensity $I_{n,\,n'}$ is usually expressed in terms of a reference intensity, generally I (Hβ). The level populations and intensities of the most important line series of hydrogen and singly ionized helium have been computed for a wide range of electron temperatures and densities, and for both Case A and Case B. Full results will be placed in the library of the Royal Astronomical Society. We restrict the following results to Case B and $n \leqslant 40$. Table I lists the intensities of the Balmer lines of H I, $I_{n,\,2}$, relative to the intensity of the H(β) line $I_{4,\,2}$(H I) = 100. The intensities of the Pickering line $I_{n,\,4}$ of He II relative to $I_{4,\,3}$(He II) = 100 are presented in Table II. At large densities, the calculations begin at $n_c \leqslant 40$. Intensities for $n > n_c$ are calculated assuming l-degeneracy (Paper I) and are presented in *italics*. At lower temperatures the effects of neglecting collisional $n \rightarrow n'$ $(n' \neq n \pm 1)$ transition are more important and a discontinuity in the two sets of calculations may result. The n-method intensities would represent an upper limit to the correct values.

The ratio of the intensities of two transitions from the same upper level is only slowly varying with the value of n for the upper level. Unlike the n-method intensities they are also slowly varying with electron temperature and density. Table III lists the ratios of the Paschen and Balmer line intensities of H I, $I_{n,\,3}/I_{n,\,2}$, for n = 5(5)40 and the same range of electron temperatures and densities. The ratios of the Pickering and Pfund line intensities of He II, $I_{n,\,5}/I_{n,\,4}$ are similarly listed in Table IV. Table V presents the effective recombination coefficients (cm^3 s^{-1}) of the two reference lines, $\alpha_{4\rightarrow 2}$(H I) and $\alpha_{4\rightarrow 3}$(He II), and also of $\alpha_{3\rightarrow 2}$(He II) and $\alpha_{5\rightarrow 3}$(He II). These lines have recently been detected in the spectra of quasars and gaseous nebulae.

The atomic data is computed to an accuracy sufficient to give intensities to within 1 per cent. If (4.1) indicates $n_c > 40$, errors will be introduced by com-

TABLE I

Hydrogen–Balmer line intensities relative to $I_{4,\,2}$(H I) = 100.

$T_e = 5\cdot10^3\,°$K

	N_e (cm^{-3})					N_e (cm^{-3})			
n	10^2	10^4	10^5	10^6	n	10^2	10^4	10^5	10^6
3	303.2	300.3	296.8	291.9	22	0.4980	0.6698	0.9079	1.100
4	100.0	100.0	100.0	100.0	23	0.4379	0.6152	0.8244	1.012
5	45.85	45.98	46.14	46.47	24	0.3879	0.5698	0.7508	0.9394
6	25.16	25.25	25.39	25.76	25	0.3454	0.5285	0.6855	0.8772
7	15.41	15.48	15.60	16.05	26	0.3095	0.4925	0.6287	0.8211
8	10.18	10.23	10.36	10.92	27	0.2786	0.4588	0.5792	0.7685
9	7.097	7.141	7.281	7.939	28	0.2524	0.4283	0.5368	0.7185
10	5.157	5.200	5.377	6.111	29	0.2295	0.3994	0.5001	0.6710
11	3.871	3.916	4.127	4.896	30	0.2103	0.3730	0.4683	0.6268
12	2.983	3.036	3.285	4.066	31	0.1932	0.3480	0.4402	*0.5719*
13	2.349	2.409	2.689	3.442	32	0.1787	0.3251	0.4152	*0.5273*
14	1.885	1.958	2.267	2.960	33	0.1656	0.3037	0.3924	*0.4866*
15	1.536	1.622	1.947	2.561	34	0.1545	0.2841	0.3715	*0.4495*
16	1.268	1.371	1.708	2.230	35	0.1443	0.2661	0.3528	*0.4156*
17	1.060	1.175	1.515	1.948	36	0.1356	0.2498	*0.3348*	*0.3847*
18	0.8958	1.025	1.359	1.713	37	0.1275	0.2350	*0.3147*	*0.3566*
19	0.7641	0.9047	1.224	1.513	38	0.1208	0.2218	*0.2959*	*0.3309*
20	0.6575	0.8110	1.108	1.347	39	0.1144	0.2101	*0.2783*	*0.3075*
21	0.4980	0.7324	1.003	1.210	40	0.1090	0.2204	*0.2618*	*0.2861*

Downloaded from https://academic.oup.com/mnras/article/153/4/471/2604558 by guest on 20 August 2022

© Royal Astronomical Society • Provided by the NASA Astrophysics Data System

1971MNRAS.153..471B

TABLE I—*continued*

$T_e = 10^4$°K

n	N_e (cm^{-3}) 10^2	10^4	10^5	10^6	n	N_e (cm^{-3}) 10^2	10^4	10^5	10^6
3	285.9	284.7	283.1	280.7	22	0.4992	0.5942	0.7180	0.8228
4	100.0	100.0	100.0	100.0	23	0.4379	0.5340	0.6437	0.7428
5	46.85	46.90	46.98	47.14	24	0.3868	0.4840	0.5796	0.6760
6	25.91	25.95	26.01	26.22	25	0.3429	0.4402	0.5235	0.6185
7	15.91	15.94	16.00	16.28	26	0.3069	0.4028	0.4750	0.5682
8	10.51	10.53	10.60	10.96	27	0.2752	0.3691	0.4327	0.5230
9	7.306	7.335	7.417	7.832	28	0.2484	0.3396	0.3962	0.4821
10	5.304	5.326	5.436	5.884	29	0.2249	0.3128	0.3643	0.4449
11	3.975	3.997	4.131	4.574	30	0.2050	0.2889	0.3365	0.4112
12	3.055	3.085	3.243	3.674	31	0.1872	0.2670	0.3121	*0.3834*
13	2.401	2.436	2.608	3.011	32	0.1720	0.2473	0.2904	*0.3526*
14	1.921	1.967	2.149	2.517	33	0.1584	0.2292	0.2709	*0.3247*
15	1.562	1.616	1.800	2.127	34	0.1465	0.2129	0.2534	*0.2995*
16	1.288	1.352	1.536	1.817	35	0.1357	0.1980	0.2378	*0.2765*
17	1.074	1.145	1.325	1.563	36	0.1263	0.1844	*0.2288*	*0.2557*
18	0.9057	0.9845	1.158	1.354	37	0.1177	0.1724	*0.2138*	*0.2368*
19	0.7709	0.8545	1.019	1.181	38	0.1102	0.1615	*0.2001*	*0.2196*
20	0.6620	0.7510	0.9037	1.038	39	0.1032	0.1514	*0.1874*	*0.2040*
21	0.5727	0.6645	0.8045	0.9196	40	0.0971	0.1427	*0.1757*	*0.1897*

$T_e = 2.10^4$°K

n	N_e (cm^{-3}) 10^2	10^4	10^5	10^6	n	N_e (cm^{-3}) 10^2	10^4	10^5	10^6
3	274.4	274.0	273.2	272.4	22	0.4984	0.5482	0.5942	0.6364
4	100.0	100.0	100.0	100.0	23	0.4366	0.4846	0.5260	0.5658
5	47.55	47.56	47.58	47.64	24	0.3849	0.4315	0.4681	0.5065
6	26.43	26.44	26.46	26.56	25	0.3411	0.3857	0.4183	0.4561
7	16.26	16.26	16.28	16.44	26	0.3041	0.3470	0.3755	0.4126
8	10.73	10.73	10.76	10.99	27	0.2722	0.3131	0.3383	0.3747
9	7.460	7.462	7.505	7.764	28	0.2450	0.2839	0.3063	0.3413
10	5.401	5.405	5.472	5.737	29	0.2213	0.2581	0.2784	0.3116
11	4.038	4.046	4.130	4.367	30	0.2009	0.2356	0.2541	0.2853
12	3.099	3.113	3.212	3.414	31	0.1830	0.2155	0.2329	*0.2706*
13	2.430	2.450	2.554	2.722	32	0.1674	0.1978	0.2142	*0.2479*
14	1.942	1.969	2.075	2.214	33	0.1535	0.1818	0.1977	*0.2275*
15	1.576	1.610	1.708	1.827	34	0.1413	0.1676	0.1831	*0.2093*
16	1.297	1.338	1.427	1.528	35	0.1302	0.1547	*0.1701*	*0.1928*
17	1.081	1.125	1.205	1.291	36	0.1205	0.1433	*0.1656*	*0.1779*
18	0.9097	0.9583	1.029	1.102	37	0.1116	0.1329	*0.1538*	*0.1645*
19	0.7732	0.8229	0.8866	0.9487	38	0.1037	0.1236	*0.1432*	*0.1524*
20	0.6629	0.7140	0.7710	0.8246	39	0.0965	0.1151	*0.1334*	*0.1413*
21	0.5727	0.6230	0.6745	0.7226	40	0.0900	0.1076	*0.1246*	*0.1313*

mencing the calculations at $n = 40$. Trial calculations, using $n_c = 50$ indicate that any errors in the intensities will be less than 1 per cent for $n < 40$. The largest uncertainties will arise in the cross-sections. Since the cross-sections enter the calculations as products of cross-sections and electron densities, we may estimate the errors in the intensities by considering the variation of intensity with N_e. Assuming a maximum error of 10 per cent in the cross-sections, maximum errors of 1 per cent rising to 2 per cent for the lower temperatures are estimated.

Downloaded from https://academic.oup.com/mnras/article/153/4/471/2604558 by guest on 20 August 2022

© Royal Astronomical Society • Provided by the NASA Astrophysics Data System

1971MNRAS.153..471B

6. ASTROPHYSICAL APPLICATIONS

The line intensities of the spectra of many nebulae are affected by selectively absorbing material in the line of sight. Denoting observed and corrected intensities by $I_0(\lambda)$ and $I_c(\lambda)$ respectively, we have

$$\log_{10} I_c(\lambda) = \log_{10} I_0(\lambda) + cf(\lambda) \tag{6.1}$$

where $f(\lambda)$ is a known function, tabulated by Burgess (1958), and c is an adjustable parameter, known as the reddening constant. It is most accurately determined by comparing theoretical and experimental values of the intensity ratios of Paschen and Balmer lines arising from the same upper state.

We restrict the analysis to the hydrogen line spectrum of NGC 7662, a well observed bright planetary nebula, and one which has received considerable attention in theoretical studies (Seaton 1960; Pengelly 1964). The photoelectric (Pe) observations of O'Dell (1963) are used for the Paschen lines P6 and P7 and the Balmer lines H3–H6, and the photographic (Pg) intensities of Aller, Kaler & Bowen (1966) for the Balmer lines H5–H30. In the latter measurements, the intensities are matched to the photoelectric intensities for the low Balmer lines. Table VI lists the transitions and observed intensities. Assuming Case B, $T_e = 10^4$°K and $N_e = 10^4\ \mathrm{cm}^{-3}$, c is calculated using H6, H7, P6 and P7, and column 5 lists the ratio of the theoretical intensities I_R to the corrected intensities I_c. Except for the strong Balmer lines, the agreement between theory and experiment is very poor. For comparison, column 6 lists the ratios using the degenerate intensities of Paper I. The agreement is improved for $n > 7$ but worse for the stronger and better observed lines.

The results are insensitive to electron temperature, while Saraph & Seaton (1970) find $N_e = 6{\cdot}0\ 10^3\ \mathrm{cm}^{-3}$, at which density equation (1.1) is inapplicable.

TABLE II

He^+–Pickering line intensities relative to $I_{4,\,3}$(He II) = 100.

$T_e = 5{\cdot}10^3$°K

	N_e (cm^{-3})				N_e (cm^{-3})		
n	10^4	10^5	10^6	n	10^4	10^5	10^6
5	27.85	28.49	28.80	23	0.2894	0.2035	0.1737
6	13.57	13.39	13.30	24	0.2688	0.1859	0.1545
7	7.649	7.423	7.311	25	0.2504	0.1715	0.1383
8	4.794	4.610	4.522	26	0.2335	0.2590	0.1247
9	3.234	3.089	3.025	27	0.2180	0.1484	0.1132
10	2.303	2.187	2.139	28	0.2036	0.1393	0.1034
11	1.710	1.614	1.576	29	0.1904	0.1313	0.0951
12	1.315	1.230	1.199	30	0.1781	0.1242	0.0880
13	1.041	0.9620	0.9359	31	0.1669	0.1178	0.0816
14	0.8471	0.7690	0.7462	32	0.1566	0.1120	0.0765
15	0.7060	0.6265	0.6056	33	0.1472	0.1065	0.0719
16	0.6012	0.5191	0.4990	34	0.1387	0.1014	0.0678
17	0.5216	0.4367	0.4166	35	0.1312	0.0965	0.0643
18	0.4593	0.3726	0.3519	36	0.1247	0.0919	0.0610
19	0.4106	0.3223	0.3003	37	0.1192	0.0874	0.0581
20	0.3715	0.2814	0.2587	38	0.1147	0.0831	0.0555
21	0.3396	0.2505	0.2248	39	0.1115	0.0790	0.0530
22	0.3127	0.2246	0.1969	40	0.1099	0.0746	0.0508

Downloaded from https://academic.oup.com/mnras/article/153/4/471/2604558 by guest on 20 August 2022

© Royal Astronomical Society • Provided by the NASA Astrophysics Data System

1971MNRAS.153..471B

TABLE II—*continued*

$T_e = 10^4\,°K$

n	N_e (cm^{-3}) 10^4	10^5	10^6	n	N_e (cm^{-3}) 10^4	10^5	10^6
5	24.46	26.90	27.07	23	0.2658	0.2090	0.1899
6	13.69	13.59	13.56	24	0.2436	0.1882	0.1690
7	7.958	7.820	7.764	25	0.2241	0.1709	0.1505
8	5.074	4.957	4.909	26	0.2067	0.1560	0.1348
9	3.547	3.364	3.326	27	0.1911	0.1434	0.1215
10	2.474	2.400	2.370	28	0.1770	0.1325	0.1100
11	1.840	1.778	1.755	29	0.1640	0.1231	0.1002
12	1.412	1.358	1.339	30	0.1523	0.1149	0.0918
13	1.112	1.063	1.047	31	0.1416	0.1076	0.0845
14	0.8973	0.8492	0.8351	32	0.1319	0.1010	0.0781
15	0.7393	0.6905	0.6776	33	0.1230	0.0951	0.0725
16	0·6207	0·5703	0·5580	34	0·1150	0·0896	0·0676
17	0·5302	0·4774	0·4653	35	0·1079	0·0845	0·0632
18	0·4590	0·4043	0·3924	36	0·1015	0·0798	0·0594
19	0·4032	0·3472	0·3342	37	0·0959	0·0754	0·0559
20	0·3583	0·3038	0·2872	38	0·0910	0·0712	0·0527
21	0·3219	0·2640	0·2479	39	0·0869	0·0673	0·0499
22	0·2915	0·2338	0·2172	40	0·0837	0·0633	0·0473

$T_e = 2\cdot10^4\,°K$

n	N_e (cm^{-3}) 10^4	10^5	10^6	n	N_e (cm^{-3}) 10^4	10^5	10^6
5	24·93	25·21	25·30	23	0·2508	0·2162	0·2070
6	13·66	13·62	13·61	24	0·2268	0·1927	0·1826
7	8·187	8·109	8·088	25	0·2062	0·1729	0·1620
8	5·310	5·242	5·221	26	0·1882	0·1561	0·1445
9	3·645	3·598	3·581	27	0·1724	0·1418	0·1296
10	2·629	2·585	2·571	28	0·1582	0·1295	0·1168
11	1·960	1·923	1·912	29	0·1455	0·1188	0·1057
12	1·503	1·472	1·463	30	0·1341	0·1096	0·0961
13	1·181	1·154	1·146	31	0·1238	0·1015	0·0878
14	0·9479	0·9216	0·9148	32	0·1145	0·0942	0·0805
15	0·7750	0·7487	0·7425	33	0·1062	0·0878	0·0741
16	0·6443	0·6171	0·6112	34	0·0986	0·0820	0·0685
17	0·5440	0·5152	0·5094	35	0·0918	0·0767	0·0635
18	0·4651	0·4352	0·4293	36	0·0857	0·0718	0·0591
19	0·4029	0·3715	0·3651	37	0·0803	0·0674	0·0551
20	0·3529	0·3202	0·3133	38	0·0754	0·0633	0·0516
21	0·3125	0·2785	0·2710	39	0·0712	0·0594	0·0484
22	0·2789	0·2443	0·2361	40	0·0675	0·0557	0·0455

Since there is no evidence of appreciable amounts of dust within the emitting region, we are led to consider, once more, the observational accuracies.

The photoelectric observations are such that all the lines are observed for the same length of time, and hence such that all line intensities contain the same absolute errors due to instrument noise (O'Dell, private communication). The usual procedure in comparing theory with observations has been to equate observed and calculated intensities for one particular line, normally taken to be Hβ. A better procedure is to make a least squares fit for all the lines observed photoelectrically. Two parameters are involved; a parameter b to allow for the fact that the intensities

Downloaded from https://academic.oup.com/mnras/article/153/4/471/2604558 by guest on 20 August 2022

© Royal Astronomical Society • Provided by the NASA Astrophysics Data System

1971MNRAS.153..471B

TABLE III

Hydrogen–Paschen/Balmer intensity ratios.

$T_e = 5\cdot10^3$ °K

n	N_e (cm^{-3}) 10^2	10^4	10^5	10^6	n	N_e (cm^{-3}) 10^2	10^4	10^5	10^6
5	0·401	0·395	0·388	0·376	25	0·368	0·327	0·310	0·307
10	0·379	0·376	0·368	0·345	30	0·362	0·315	0·308	0·307
15	0·374	0·365	0·343	0·316	35	0·354	0·310	0·307	0·307
20	0·372	0·346	0·319	0·308	40	0·343	0·308	0·307	0·307

$T_e = 10^4$ °K

n	N_e (cm^{-3}) 10^2	10^4	10^5	10^6	n	N_e (cm^{-3}) 10^2	10^4	10^5	10^6
5	0·348	0·346	0·342	0·336	25	0·344	0·320	0·310	0·307
10	0·347	0·346	0·341	0·326	30	0·339	0·313	0·308	0·307
15	0·346	0·340	0·326	0·313	35	0·333	0·310	0·307	0·307
20	0·346	0·328	0·315	0·308	40	0·327	0·308	0·307	0·307

$T_e = 2\cdot10^4$ °K

n	N_e (cm^{-3}) 10^2	10^4	10^5	10^6	n	N_e (cm^{-3}) 10^2	10^4	10^5	10^6
5	0·305	0·304	0·303	0·300	25	0·319	0·309	0·308	0·307
10	0·318	0·317	0·314	0·304	30	0·315	0·309	0·307	0·307
15	0·320	0·315	0·309	0·307	35	0·311	0·308	0·307	0·307
20	0·320	0·310	0·308	0·307	40	0·309	0·307	0·307	0·307

TABLE IV

He^+–Pickering/Pfund line intensity ratios.

$T_e = 5\cdot10^3$ °K

n	N_e (cm^{-3}) 10^4	10^5	10^6	n	N_e (cm^{-3}) 10^4	10^5	10^6
6	0·779	0·759	0·718	25	0·651	0·608	0·544
10	0·705	0·732	0·683	30	0·633	0·569	0·528
15	0·674	0·668	0·642	35	0·604	0·543	0·522
20	0·661	0·645	0·586	40	0·575	0·529	0·520

$T_e = 10^4$ °K

n	N_e (cm^{-3}) 10^4	10^5	10^6	n	N_e (cm^{-3}) 10^4	10^5	10^6
6	0·688	0·679	0·654	25	0·626	0·596	0·544
10	0·662	0·657	0·648	30	0·614	0·565	0·528
15	0·642	0·638	0·620	35	0·593	0·542	0·522
20	0·634	0·623	0·579	40	0·571	0·530	0·520

$T_e = 2\cdot10^4$ °K

n	N_e (cm^{-3}) 10^4	10^5	10^6	n	N_e (cm^{-3}) 10^4	10^5	10^6
6	0·613	0·610	0·596	25	0·599	0·580	0·541
10	0·619	0·617	0·611	30	0·591	0·558	0·527
15	0·608	0·606	0·595	35	0·578	0·540	0·522
20	0·604	0·597	0·567	40	0·562	0·529	0·520

Downloaded from https://academic.oup.com/mnras/article/153/4/471/2604558 by guest on 20 August 2022

© Royal Astronomical Society • Provided by the NASA Astrophysics Data System

1971MNRAS.153..471B

TABLE V

(*a*) *Effective recombination coefficients* $\alpha_{4\to2}$ *for hydrogen.*
(*b*) *Effective recombination coefficients* $\alpha_{4\to3}$ *for singly ionized helium.*
(*c*) *Effective recombination coefficients* $\alpha_{3\to2}$ *for singly ionized helium.*
(*d*) *Effective recombination coefficients* $\alpha_{5\to3}$ *for singly ionized helium.*

T_e (°K) =	5.10^3	10^4	2.10^4
(a)			
N_e (cm^{-3})	$10^{14}\,\alpha_{4\to2}$	$10^{14}\,\alpha_{4\to2}$	$10^{14}\,\alpha_{4\to2}$
10^2	5·391	3·023	1·610
10^4	5·443	3·036	1·612
10^5	5·504	3·049	1·615
10^6	5·592	3·069	1·618
(b)			
N_e (cm^{-3})	$10^{14}\,\alpha_{4\to3}$	$10^{14}\,\alpha_{4\to3}$	$10^{14}\,\alpha_{4\to3}$
10^4	69·15	34·92	16·90
10^5	68·79	34·77	16·86
10^6	66·91	33·95	16·57
(c)			
N_e (cm^{-3})	$10^{14}\,\alpha_{3\to2}$	$10^{14}\,\alpha_{3\to2}$	$10^{14}\,\alpha_{3\to2}$
10^4	143·8	80·68	44·08
10^5	145·2	81·02	44·16
10^6	145·6	80·88	44·06
(d)			
N_e (cm^{-3})	$10^{14}\,\alpha_{5\to3}$	$10^{14}\,\alpha_{5\to3}$	$10^{14}\,\alpha_{5\to3}$
10^4	17·89	9·911	5·217
10^5	18·12	9·957	5·224
10^6	18·26	9·946	5·205

are on an arbitrary scale; and a parameter c to allow for reddening. We therefore vary b and c so as to minimize

$$F(b, c) = \sum_n [I_0 - b\ 10^{-cf(\lambda_n)}\, I_R]^2. \tag{6.2}$$

For $T_e = 10^4$°K and $N_e = 10^4\,\mathrm{cm}^{-3}$, and giving equal weights to the photoelectric observations of P5, P6 and H3–H6 (we neglect P9 and P10 due to possible blending with OH emission), we find $b = 0{\cdot}977$ and $c = 0{\cdot}228$. The intensity difference

$$\Delta I_n = I_0 - b\ 10^{-cf(\lambda_n)}\, I_R \tag{6.3}$$

is plotted in Fig. 3 as a function of upper quantum number, n. Intensities are relative to $I_0\,(H\beta) = 100$.

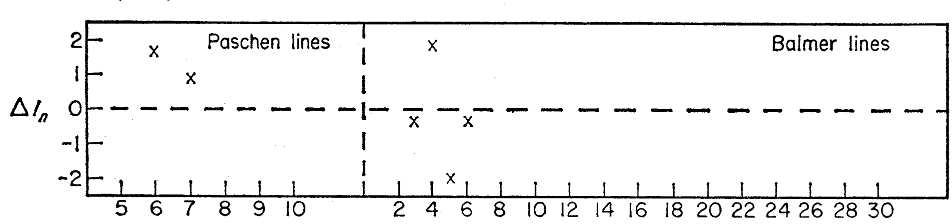

FIG. 3. *The differences between the calculated and theoretical intensities of the photoelectric observations of hydrogen lines of NGC 7662 (I_0 ($H\beta$) = 100).*

Downloaded from https://academic.oup.com/mnras/article/153/4/471/2604558 by guest on 20 August 2022

© Royal Astronomical Society • Provided by the NASA Astrophysics Data System

1971MNRAS.153..471B

TABLE VI

Comparison of theory and observations for NGC 7662.

n	n'	Method	I_0	$(I_R/I_c)_{nl}$	$(I_R/I_c)_n$	R_n	$n^3 I_{n,\ n}$l
6	3	Pe	16·2	—	—	1·181	—
7	3	Pe	9·55	—	—	1·158	—
3	2	Pe	339	1·06	1·05	0·999	9·15
4	2	Pe	100	1·00	1·00	1·018	6·40
5	2	Pe	40·7	1·06	1·12	0·956	5·09
6	2	Pe	22·4	1·01	1·13	0·990	4·84
5	2	Pg	44·3	0·97	1·03	1·041	5·54
6	2	Pg	20·0	1·14	1·27	0·884	4·32
7	2	Pg	14·6	0·93	1·08	1·076	5·01
9	2	Pg	8·00	0·76	0·94	1·313	5·83
10	2	Pg	6·70	0·65	0·83	1·525	6·70
11	2	Pg	4·40	0·74	0·97	1·342	5·86
12	2	Pg	3·50	0·72	0·95	1·388	6·05
13	2	Pg	3·10	0·64	0·85	1·562	6·81
15	2	Pg	2·10	0·62	0·84	1·602	7·09
16	2	Pg	1·72	0·63	0·85	1·571	7·05
17	2	Pg	1·49	0·62	0·83	1·609	7·32
18	2	Pg	1·28	0·62	0·82	1·608	7·46
19	2	Pg	0·94	0·73	0·96	1·362	6·65
20	2	Pg	0·86	0·70	0·91	1·420	6·88
21	2	Pg	0·72	0·74	0·94	1·343	6·67
22	2	Pg	0·68	0·70	0·88	1·421	7·24
23	2	Pg	0·53	0·89	0·99	1·233	6·45
24	2	Pg	0·49	0·79	0·95	1·258	6·77
25	2	Pg	0·39	0·90	1·06	1·102	6·09
26	2	Pg	0·43	0·75	0·87	1·327	7·56
27	2	Pg	0·38	0·77	0·88	1·281	7·48
28	2	Pg	0·37	0·73	0·82	1·354	8·12
29	2	Pg	0·39	0·64	0·70	1·551	9·52
30	2	Pg	0·31	0·74	0·80	1·335	8·37

Column 7 of Table VI lists the quantity R_n for all observations, where

$$R_n = I_0/I_R b\ 10^{-cf(\lambda_n)}. \tag{6.4}$$

In Fig. 4, values of R_n are plotted as a function of upper quantum number, n, and on the same horizontal scale as in Fig. 3. All photoelectric observations give values of R_n very close to unity (less weight is given in this plot to the Paschen lines since they are of weak intensity) and certainly unity within experimental error. The photographic observations, however, are suspect. Apart from the stronger Balmer lines which are normalized to the photoelectric observations, the departures from $R_n = 1$ are much greater than experimental error would suggest and always such that $R_n > 1$. From equation (5.1) we obtain

$$n^3 I_{n,\ n'} \xrightarrow{n\to\infty} K b_n \tag{6.5}$$

where K is a constant and $b_n \to 1$. Column 8 lists the experimental values of this quantity. There is considerable scatter and certainly no asymptotic value for the weak photographic lines.

Downloaded from https://academic.oup.com/mnras/article/153/4/471/2604558 by guest on 20 August 2022

© Royal Astronomical Society • Provided by the NASA Astrophysics Data System

1971MNRAS.153..471B

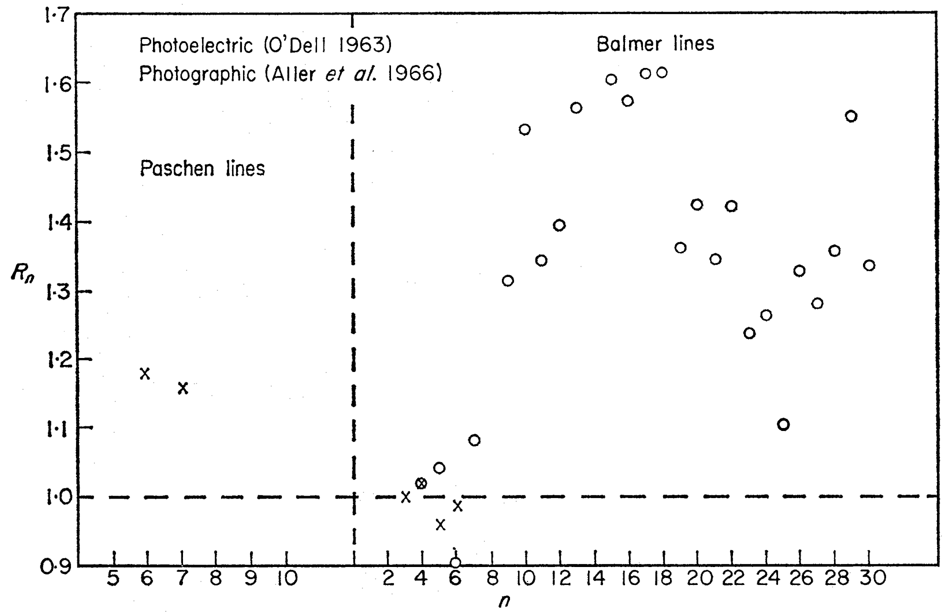

FIG. 4. *Plot of R_n v. n for observations of NGC* 7662. Photoelectric (×); photographic (○).

7. CONCLUSIONS

Recombination spectra have been calculated making full allowance for collisional redistribution of angular momentum and energy. The line intensities, while considerably different from those of Pengelly (1964), do not agree with the photographic observations. There is evidence that the photographic observations of the weak lines contain systematic errors. Further evidence is provided by Miller (1971), who has recently made photoelectric observations of H15–H18 in NGC 7027 and NGC 7662. NGC 7027 has always shown the largest deviation from theory (Seaton 1960; Kaler 1966), the high Balmer lines, previously measured photographically, being three or four times too strong. The new measurements indicate that the discrepancy is less than 40 per cent when compared with the same theory. For NGC 7662 the photoelectric intensities are 30 per cent smaller than the equivalent photographic intensities of Aller (1963) and the agreement with the above theory is very good. There is clearly a need for extending the range of photoelectric measurements, and for re-examining the methods of obtaining photographic intensities of weak lines.

ACKNOWLEDGMENTS

I should like to express my sincere thanks to Professor M. J. Seaton for his constant encouragement and guidance in this work. It is a pleasure to thank Professor C. R. O'Dell for much useful advice, W. G. Mathews & J. S. Miller for communicating their results prior to publication and P. J. Storey for many helpful discussions. The author acknowledges the receipt of an S.R.C. studentship, and the award of an I.B.M. Fellowship during the tenure of which this work was completed.

Physics Department, University College, London

Received in original form 1970 *December* 21

Downloaded from https://academic.oup.com/mnras/article/153/4/471/2604558 by guest on 20 August 2022

© Royal Astronomical Society • Provided by the NASA Astrophysics Data System

1971MNRAS.153..471B

REFERENCES

Aller, L. H., Bowen, I. S. & Minkowski, R., 1955. *Astrophys. J.*, **122**, 62.
Aller, L. H., Bowen, I. S. & Wilson, O. C., 1963. *Astrophys. J.*, **138**, 1013.
Aller, L. H., Kaler, J. B. & Bowen, I. S., 1966. *Astrophys. J.*, **144**, 291.
Baker, J. G. & Menzel, D. H., 1938. *Astrophys. J.*, **88**, 52.
Brocklehurst, M., 1970. *Mon. Not. R. astr. Soc.*, **148**, 417.
Burgess, A., 1958. *Mon. Not. R. astr. Soc.*, **118**, 417.
Burgess, A., 1965. *Mem. R. astr. Soc.*, **69**, 1.
Burgess, A. & Seaton, M. J., 1960. *Mon. Not. R. astr. Soc.*, **120**, 121.
Churchwell, E. & Mezger, P. G., 1970. *Astrophys. Lett.*, **5**, 227.
Dyson, J. E., 1969. *Astrophys. J.*, **155**, 4.
Gordon, W., 1929. *Ann. Phys.*, **2**, 1031.
Green, L. C., Rush, P. P. & Chandler, C. D., 1957. *Astrophys. J. Suppl.*, **3**, 37.
Kaler, J. B., 1966. *Astrophys. J.*, **143**, 722.
Kaler, J. B., 1968. *Astrophys. Lett.*, **1**, 227.
Miller, J. S., 1971. *Astrophys. J. Lett.*, **165**, L101.
O'Dell, C. R., 1963. *Astrophys. J.*, **138**, 1018.
Osterbrock, D. E., 1962. *Astrophys. J.*, **135**, 195.
Pengelly, R. M., 1964. *Mon. Not. R. astr. Soc.*, **127**, 145.
Pengelly, R. M. & Seaton, M. J., 1964. *Mon. Not. R. astr. Soc.*, **127**, 165.
Plaskett, H. H., 1928. *Publ. Dom. astrophys. Obs. Victoria*, **4**, 187.
Saraph, H. E., 1964. *Proc. Phys. Soc.*, **83**, 763.
Saraph, H. E. & Seaton, M. J., 1970. *Mon. Not. R. astr. Soc.*, **148**, 367.
Seaton, M. J., 1959. *Mon. Not. R. astr. Soc.*, **119**, 90.
Seaton, M. J., 1960. *Rep. prog. Phys.*, **23**, 113.
Seaton, M. J., 1962. *Proc. Phys. Soc.*, **79**, 1105.
Seaton, M. J., 1964. *Mon. Not. R. astr. Soc.*, **127**, 177.
Spitzer, I., 1956. *Physics of Fully Ionized Gases*, Interscience, New York.

Downloaded from https://academic.oup.com/mnras/article/153/4/471/2604558 by guest on 20 August 2022

© Royal Astronomical Society • Provided by the NASA Astrophysics Data System